Journal Pre-proofs

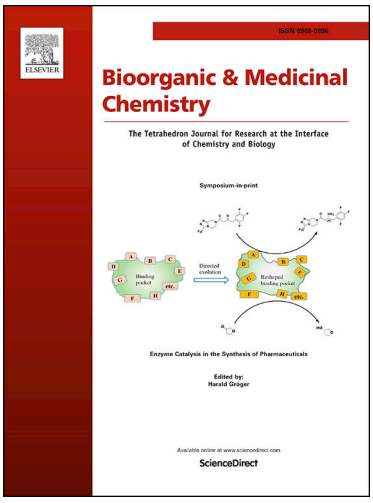

Design, synthesis and acaricidal activities of Cyflumetofen analogues based on carbon-silicon isosteric replacement

Cong Zhou, Jiagao Cheng, Ryan Beadle, Fergus G Earley, Zhong Li, Peter Maienfisch

PII: S0968-0896(20)30335-7
DOI: https://doi.org/10.1016/j.bmc.2020.115509
Reference: BMC 115509

To appear in: *Bioorganic & Medicinal Chemistry*

Received Date: 10 January 2020
Revised Date: 7 April 2020
Accepted Date: 14 April 2020

Please cite this article as: C. Zhou, J. Cheng, R. Beadle, F.G. Earley, Z. Li, P. Maienfisch, Design, synthesis and acaricidal activities of Cyflumetofen analogues based on carbon-silicon isosteric replacement, *Bioorganic & Medicinal Chemistry* (2020), doi: https://doi.org/10.1016/j.bmc.2020.115509

Design, synthesis and acaricidal activities of Cyflumetofen analogues based on carbon-silicon isosteric replacement

Cong Zhou[a], Jiagao Cheng[a,], Ryan Beadle[b,d], Fergus G Earley[b], Zhong Li[a], Peter Maienfisch[a,c,]**

[a]*Shanghai Key Laboratory of Chemical Biology, School of Pharmacy, East China University of Science and Technology, Shanghai, 200237, China*

[b]*Syngenta Crop Protection AG, Jealott's Hill Research Centre, Bracknell, Berkshire, UK*

[c]*Syngenta Crop Protection AG, Schwarzwaldallee 215, CH-4002 Basel, Switzerland*

[d]*Current address: Department of Biochemistry, University of York, US*

* Corresponding authors:

Peter Maienfisch, E-mail: peter.maienfisch@syngenta.com;

Jiagao Cheng, E-mail: jgcheng@ecust.edu.cn

ABSTRACT

The application of a carbon-silicon bioisosteric replacement strategy to find new acaricides with improved properties led to the discovery of Sila-Cyflumetofen **6B**, a novel and highly potent acaricide. The essential *t*-butyl group in the *beta*-ketonitrile acaricide Cyflumetofen **6A** could be swapped with the bioisosteric trimethyl-silyl group with retention of high level acaricidal activity and favourable pharmacological properties. Sila-Cyflumetofen **6B** was found to possess similar preferred energy-minimized conformation and electrostatic potential surface compare to Cyflumetofen **6A**. Herein we also report the development and application of the first homology model of the spider mite mitochondrial electron transport complex II (succinate ubiquinone oxidoreductase; SQR) and demonstrated that the active metabolite **AB-1** of Cyflumetofen **6A** and its sila-analogue **Sila-AB-1** bind to the Qp site in same binding pose and that both compounds form two H-bonds and a cation-π interaction with Trp 165, Tyr 433 and Arg 279, respectively. Furthermore, we also developed a new mode of action test for spider mite Complex II using cytochrome c as electron acceptor and blocking its re-oxidation by addition of KCN resulting in a sensitive and convenient colorimetric assay. This new method avoids the use of non-specific artificial electron acceptors and allows to measure SQR inhibition in crude extracts of *Tetranychus urtice.* In this assay **Sila-AB-1**, the intrinsically active metabolite of Sila-Cyflumetofen, **6A** exhibited even a somewhat lower IC_{50} value than the metabolite of Cyflumetofen **AB-1**. Synthetic methodologies are described for the preparation of Sila-Cyflumetofen **6B**

and its active metabolite **Sila-AB-1** which enable an efficient synthesis of these compounds in only 5 and 4 steps, respectively, from cheap commercial starting materials. Although the value of carbon-silicon bioisosteric replacements has already be demonstrated in the past it is to the best of our knowledge the first report of a successful application in crop protection research in the last two decades.

Keywords:

Discovery of Sila-Cyflumetofen, *beta*-ketonitrile acaricide, Carbon-silicon bioisosteric replacement, succinate ubiquinone oxidoreductase, homology model, spider mite SQR inhibition

1. Introduction

Modern agrochemicals play a vital role in safeguarding and improving the production, quality, and quantity of food, feed, fiber, and fuel. With the current offerings on insecticides, herbicides, fungicides and biotechnology products together with considerable investments in research and development the global agribusiness industry contributes to growing public expectations for adequate supply of high-quality food and agricultural sustainability. Despite the current arsenal of insect control agents there is a clear demand for new innovative, safe and highly effective products mainly due to the development of resistance to existing active ingredients, pest shifts and the increasing regulatory requirements.[1]

Bioisosterism has been demonstrated to be a powerful source of chemical diversity in biological active molecules design, also has been considered as an effective approach to solve the challenges that modern agrochemicals are facing.[2-10] Furthermore applying an isosteric replacement strategy maximizes the chances for success in discovering novel modern agrochemicals. For example, Oxathiapiprolin[11-12] is the first highly-active piperidinyl thiazole isoxazolines fungicides developed by DuPont in 2015. The original hit leading to Oxathiapiprolin was identified by screening an external compound library and showed only modest preventative and weak curative fungicidal activity. A series of isosteric optimization at all parts of the original hit compound, led to strongly improved biological activity and finally to the discovery of Oxathiapiprolin, a compound introduced to the marketplace in 2015 and reportedly active at lower application rates than existing Oomycete products.

Although the carbon-silicon bioisosteric replacement strategy received increasing attention in pharmaceutical research in the last two decades,[13-20] this discovery strategy was employed to a much lesser extend in crop protection research despite past research successes leading to the fungicide Flusilazole[21-23] and the insecticide Silafluofen[2-3, 24] – products entering the market places in the late 1980s and early 1990s. Both carbon and silicon are elements in Group IV of the periodic table. They share the ability to form four covalent, tetrahedrally disposed bonds which makes silicon the ideal bioisosteric replacement for carbon.[25-26] Silicon-containing bioactive molecules designed by the strategy of carbon-silicon replacement enables to modify physicochemical properties, biological activity profile and target selectivity.[15, 27-28]

Cyflumetofen **(6A)**, is a novel *beta*-ketonitrile acaricide discovered and developed by Otsuka. The compound provides excellent control of mites and has been currently marketed in many countries around the world.[29-30] Cyflumetofen **(6A)** exhibits excellent and highly selective efficacy against a variety of mites whereas having no effect on non-targeted organisms potentially due to the procide structure.[29-31] Cyflumetofen **(6A)** is activated by de-esterification and spontaneous decarboxylation leading to **AB-1** as main metabolite and active principle which interacts with the mitochondrial electron transport complex II.[30, 32]

Mitochondrial electron transport complex II or succinate ubiquinone oxidoreductase (SQR) is an important target for acaricides and fungicides. In the last decade other novel acaricides such as Cyenopyrafen[33-35] and Pyflubumide[36-37] were developed targeting SQR. SQR has also been identified as one of the most significant targets for the

discovery of new fungicides.[38-41] Succinate dehydrogenase inhibitors (SDHI) provide broad spectrum fungicidal activities and are important tools in disease control as the numerous Complex II market products of high commercial value demonstrate. Though great achievements have been made in revealing the function and structure of SQR, neither the crystal structure of SQR from spider mites has been detected nor the binding mode of Complex II acaricides in a target species been elucidated, and therefore further research on novel acaricides is restrained.

During the optimization of Cyflumetofen **(6A)**, it was found that *tert*-butyl at *para*-position leads to the best activity.[29] In our research strategy aiming to discover novel acaricides with improved properties we considered the bioisosteric replacement of carbon by silicon as a promising approach. Many options were considered for the introduction of a silicon-containing substituent or for the integration of silicon into the molecular skeleton of Cyflumetofen **(6A)** and have ultimately selected Sila-Cyflumetofen **(6B)** as highly interesting target compound. The replacement of the *tert*-butyl group by the bioisosteric trimethysilyl moiety was expected to lead potentially to favourable changes in ligand-receptor interactions and of the pharmacology and pharmacodynamic properties by influencing the molecular conformation, electron distribution and physicochemical properties.[14, 42-45] Furthermore the introduction of silicon motifs in existing products also offers opportunities for the generation of new intellectual property (IP).[14, 25]

In this paper we report our discovery of the silicon-containing Cyflumetofen analogue **6B** as a potent new acaricide and describe its synthesis, biological activity,

physicochemical properties, enzyme inhibition and its potential surfaces. Furthermore, we discuss the binding modes within SQR in spider mites and differences between Cyflumetofen (**6A**) and its sila-analogue (**6B**) attributed to the carbon-silicon replacement.

2. Results and discussion

2.1 Synthetic Chemistry

Sila-Cyflumetofen **6B** was synthesized in 5 steps as shown in scheme 1. Key steps involved the synthesis of 4-trimethylsilyl-phenylacetonitril **3B** from 1,4-dibromobenzene **1** by *n*-BuLi mediated introduction of the trimethylsilyl group followed by Pd-catalized C-C bond formation reaction.[46] Later steps followed synthetic methodology used for the synthesis of Cyflumetofen (Scheme 1).[47] The build blocks **5A** and **5B** were synthetized by reactions of the phenylacetonitrils **3A** and **3B**, respectively, with diethyl carbonate and subsequent trans-esterification catalyzed by concentrated sulfuric acid. Finally, the benzoyl moiety in the target compounds **6A** and **6B** was introduced by reacting **5A** and **5B** with 2-trifluoromethylbenzoyl chloride. According to the reaction conditions and yields, we found that the trimethysilyl-substituent did not alter the reactivities remarkably compared to the *tert*-butyl-substituted analogues.

Cyflumetofen **6A** and Sila-Cyflumetofen **6B** are proinsecticides[31] which after hydrolytical or enzymatic activation are converted to the intrinsic active metabolites **AB-1** and its sila-analogue **Sila-AB-1**, respectively. These two compounds were

synthesized as shown in scheme 2 in order to investigate the intrinsic activity. Treatment of phenyl acetonitriles **4A** and **4B** in the presence of NaH in refluxing tetrahydrofuran with ethyl 2-(trifluoromethyl)benzoate **8** afforded **AB-1** and **Sila-AB-1**, respectively, in good yields (Scheme 2).[48-50] NMR analysis revealed that **AB-1** and **Sila-AB-1**, respectively, exist in both tautomeric forms at room temperature. In order to further confirm the structures of **AB-1** and **Sila-AB-1** their acylated derivatives **9A** and **9B** were prepared by treatment with pivaloyl chloride and triethylamine in dichloromethane and characterized.[33, 51-52]

Scheme 1:

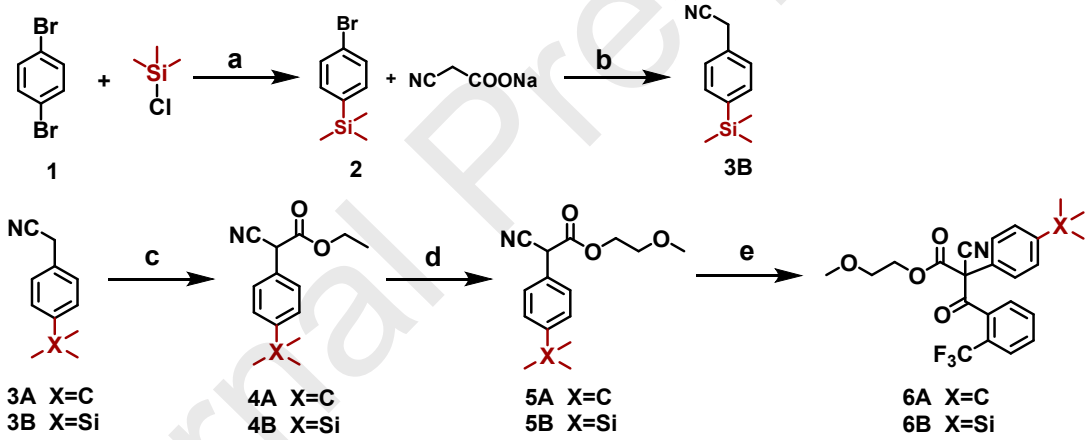

Scheme 1. Synthetic scheme of Sila-Cyflumetofen: Reagents and conditions: a. *n*-BuLi, tetrahydrofuran, -78 °C - r.t; b. 2 mol% $[Pd_2(allyl)_2Cl_2]$, 6 mol% S-Phos, mesitylene, 140 °C; c. Diethyl carbonate, NaH, tetrahydrofuran, 56 °C; d. H_2SO_4, 2-methoxyethanol, 100 °C; e. NaH, tetrahydrofuran, then 2-(trifluoromethyl)benzoyl chloride, 0 °C - r.t.

Scheme 2:

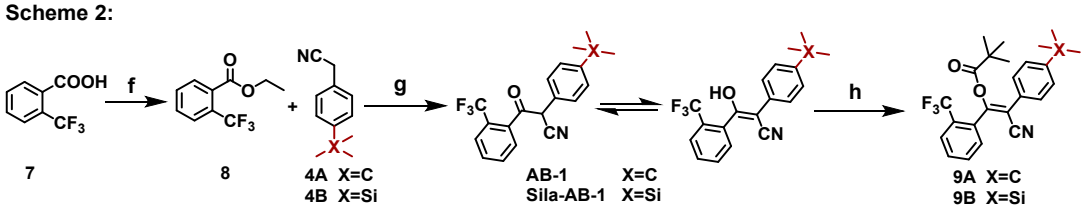

Scheme 2. Synthetic scheme of metabolites and acylated derivatives: Reagents and conditions: f.

H_2SO_4, ethanol, pressure, 120 °C; g. NaH, tetrahydrofuran, reflux; h. pivaloyl chloride, triethylamine, dichloromethane, r.t.

2.2 Acaricidal activities

The acaricidal activity of Sila-Cyflumetofen **(6B)** was tested against the two spotted spider mite (*Tetranychus urticae*). As shown in the Table 1, Sila-Cyflumetofen **(6B)** exhibited as good acaricidal activity as the parent compound at 200 and 50 ppm. At 12.5 ppm Cyfumetofen **(6A)** still showed partial activity against *T. urticae*, whereas Sila-Cyflumetofen **(6B)** was inactive. Although the silicon compound showed somewhat lower activity than its carbon counterpart, our results have proven that silicon is a valuable bioisosteric replacement for carbon with respect to the 4-*t*-Bu-phenyl moiety and can lead to a highly active acaricide. The translation of this activity to field situations and the influence of the differences in the physicochemical properties on the field performance still need to be investigated.

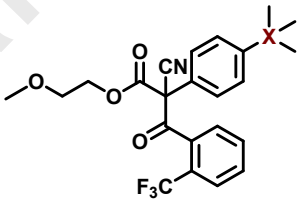

Table 1. Acaricidal activities of title compounds against *T. urticae*

	X	Acaricidal activities at concn. of (ppm)			
		200	**50**	**12.5**	**3**
Cyflumetofen 6A	C	100	100	70-100	0
Sila-Cyflumetofen 6B	Si	100	100	0	0

2.3 Enzyme inhibition

Complex II or succinate: quinone oxidoreductase (SQR) is an essential component of the tricarboxylic acid (or Krebbs) cycle and as such is required for energy conservation from the oxidation of fat and carbohydrate. It catalyzes the oxidation of succinate to fumarate, coupled to the reduction of ubiquinone to ubiquinol. Ubiquinol is re-oxidized by molecular oxygen by electron transfer through Complex III (cytochrome b/c1 complex), cytochrome c, and Complex IV (cytochrome a/a3). Complex III, Complex IV and SQR are integral components of the inner mitochondrial membrane and co-purify in mitochondrial preparations.[53]

The mode of action of Cyflumetofen, Cyenopyrafen and Pyflubumide and their analogues was determined to be SQR inhibition by comparing effects on the oxidation of succinate, pyruvate and α-glycerophosphate in polarographic assays.[30] Because such assays require relatively large amounts of mitochondrial protein, we instead used cytochrome c as electron acceptor, blocking its re-oxidation by addition of KCN. This provides a sensitive and convenient colorimetric assay that avoids the use of non-specific artificial electron acceptors[54] and allows assay of SQR inhibition in crude extracts of *Tetranychus urtice*.

Cyflumetofen is a procide requiring conversion to its active principle **AB-1** that involves carboxylesterase activity[55]. The active metabolites **AB-1** and **Sila-AB-1** of Cyflumetofen and Sila-Cyflumetofen were found to inhibit the succinate–cytochrome c oxidoreductase activity at extremely low concentrations, confirming that carbon-silicon replacement did not lead to alteration of the mode of action. The IC_{50} values of

AB-1 and the sila-analouge **Sila-AB-1** for oxidoreductase activity were 0.0025 and 0.0016 μg.ml^{-1}, respectively (Fig 1). **Sila-AB-1** exhibited slightly stronger enzyme inhibition than **AB-1** from which we can conclude that the slightly lower acaricidal activity of Sila-Cyflumetofen against *T. urticae* resulted from the changes in physicochemical properties or pharmacological and pharmacodynamic properties.

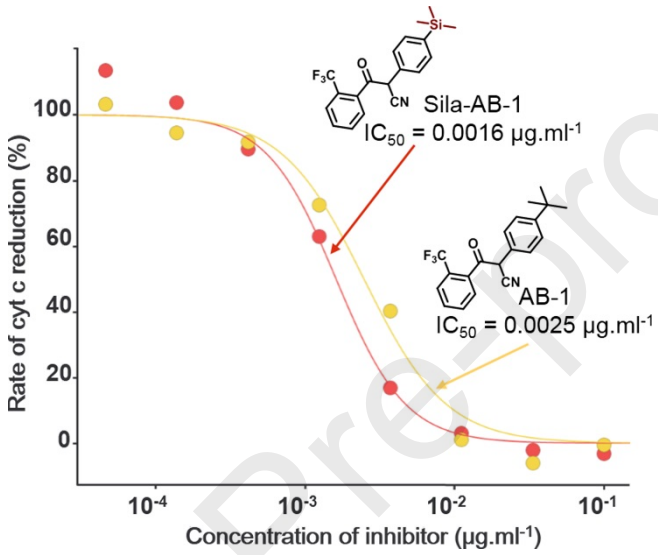

Fig. 1. Inhibition profiling of succinate-cytochrome oxidoreductase activity.

2.4 Potential Surfaces and physicochemical properties analysis

Potential surfaces and physicochemical properties including clogP, clogS and TPSA (Topological Polar Surface Area) were investigated to identify the potential changes in physicochemical properties or pharmacological and pharmacodynamic properties resulting from a carbon-silicon replacement. As shown in Fig.2 and Table 2, carbon-silicon replacement gave little difference to the preferred energy-minimized conformation, electrostatic potential surfaces and clogS values. However, Sila-Cyflumetofen (**6B**) exhibited higher lipophilicity than Cyflumetofen (**6A**) in the

carbon-silicon replacement domain according to lipophilic potential surfaces (Fig.2, c and d). The clogP value (5.40) of Sila-Cyflumetofen (**6B)** only increased about 0.28 as compared to **6B** (5.12). There was no difference in TPSA value, as carbon-silicon replacement did not alter the polar groups. Fig.2 (e) depicts the physicochemical properties of representative pesticides targeting sucking pests, mites and chewing pests. The physicochemical properties of Sila-Cyflumetofen (**6B)** are situated in the suitable range of commercial products (Fig.2, e). From the modelling and the analysis of physicochemical properties, we can conclude that carbon-silicon isosteric replacement did not result in major differences in the macroscopical characteristics confirming trimethysilyl to be an ideal bioisosteric replacement of the *tert*-butyl group.

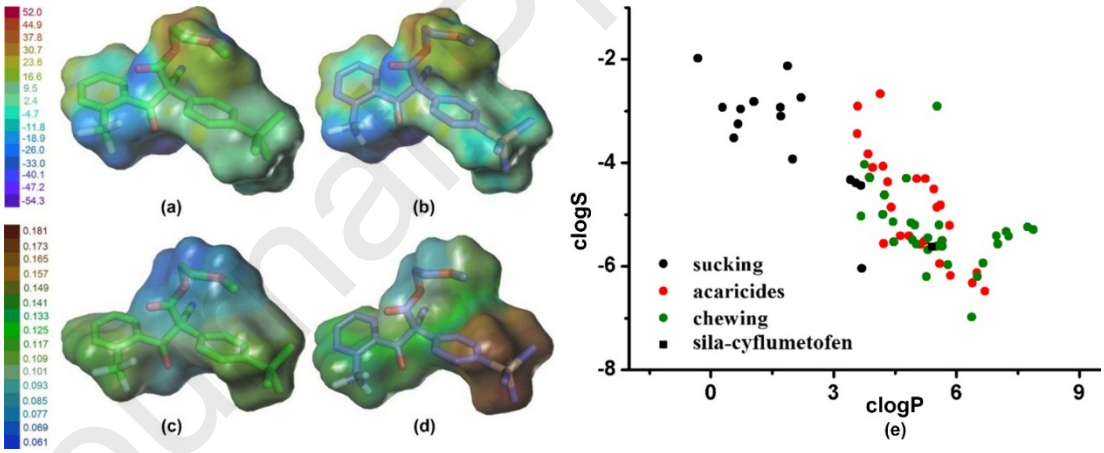

Fig. 2. Electrostatic potential surface of Cyflumetofen (a) and Sila-Cyflumetofen (b); lipophilic potential surfaces of Cyflumetofen (c) and Sila-Cyflumetofen (d); The plot of physicochemical properties for representative pesticides and Sila-Cyflumetofen (e)

Table 2. Physicochemical properties of title compounds

Compounds	physicochemical properties		
	clogP	clogS	TPSA
Cyflumetofen	5.12[a]	-5.58	76.39
Sila-Cyflumetofen	5.40	-5.62	76.39

a. The experimental value is 4.3

2.5 The Homology Model of T. cinnabarinus SQR

Up to present, the crystal structures of SQR were developed from *E.coli*[56-59], *Sus scrofa*[60-62] and *Gallus gallus*[63-64], no SQR crystal structure from spider mites has been reported. Furthermore, the binding modes of acaricides targeting SQR are still not clear, and further insights are highly desirable to enable further research on Complex II acaricides. The binding characteristics cannot be correctly simulated with the present SQR crystal structures because of different residues around the binding pocket. Computational simulations including homology modeling and molecular docking were applied to get insights into the binding modes of Cyflumetofen (**6A)** and the differences in binding modes attribute to the carbon-silicon replacement.

The amino acid sequences of *T. urticae* SQR subunits were not available from UniProt database (https://www.uniprot.org/). Therefore, the amino acid sequences of SQR subunits from carmine spider mite (*Tetranychus cinnabarinus*) were subjected to template search, to enable building a homology model. Taking the sequence identity, crystal resolution values and residue completeness into account, the crystal structure of porcine mitochondrial respiratory complex II co-crystalized with ubiquinone (PDB ID: 1ZOY[60] at 2.4 Å resolution) was selected as the template to build the 3D structure of *T. cinnabarinus* SQR. The final sequence alignment between target sequences and template used for generating the 3D model of SQR is depicted in Fig.3 (a).

The overall identity and similarity of target sequences with the template were 56.0%

and 73.3%, respectively. The quality of the established homology model was assessed by the PROCHECK Ramachandran plot,[65] Profile-3D[66] and Prosa-web z-score approaches (https://prosa.services.came.sbg.ac.at/prosa.php). In the Ramachandran plot evaluation (Fig.3, b), 91.6% of the residues were present in the most favored regions, 7.7% in the additional regions, 0.5% in the generously allowed regions, and only 0.2% in the disallowed regions. The Verify score by Profile-3D for *T. cinnabarinus* SQR structure was 221.64, which was higher than the top score 221.54. Moreover, most residues were reasonable with positive score values, and only a few residues positioned far away from the binding site regions showed small negative profile-3D values (Fig.3, d). Prosa-web z-score proves an interpretation of protein quality, the plot contains the z-scores of all experimentally determined protein chains in current PDB database. Structures from different sources (X-ray, NMR) are distinguished by different colors. The z-score of *T. cinnabarinus* SQR structure was -7.26, which was in the range of native conformations determined by NMR (Fig.3, c). The above results indicated that the homology model of *T. cinnabarinus* SQR was reliable and could be used for further molecular docking study. This is to the best of our knowledge the first report on the development of a homology model of the spider mite mitochondrial electron transport complex II (succinate ubiquinone oxidoreductase; SQR) and is expected to stimulate further research in the area of silicon-containing complex II acaricides as well as novel chemistries targeting this mode of action.

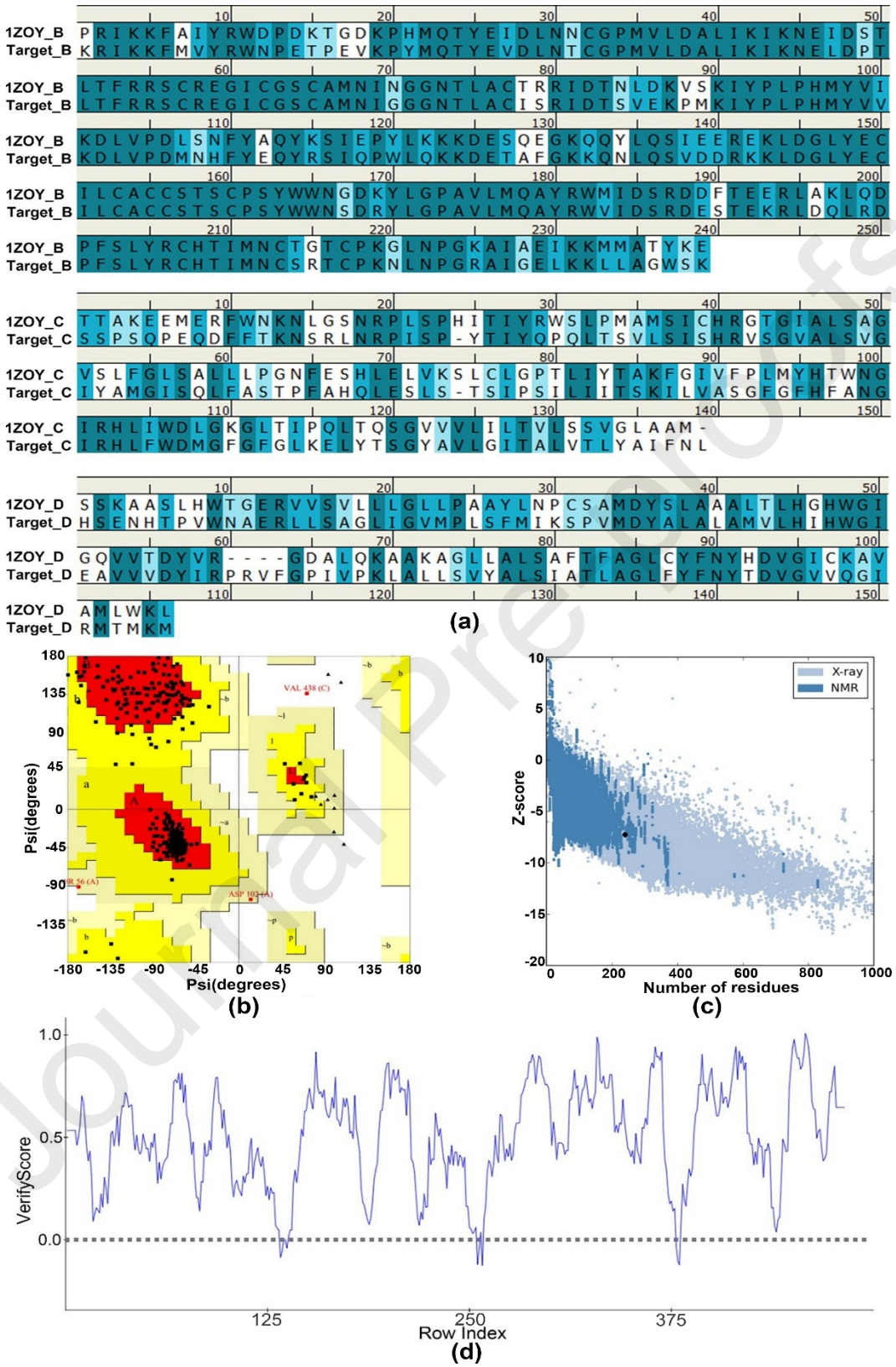

Fig. 3. Sequence alignment results of the template sequence (PDB ID: 1ZOY) with *T. cinnabarinus* SQR subunits B, C and D (UniProt ID: A0A0K1SB10, A0A0K1SB53 and A0A0K1SAS9) (a), the

Ramachandran plots (c), the Z-Score plots (c), and the Profile-3D results (d) of *T. cinnabarinus* Mitochondrial Respiratory Complex II

2.6 Binding mode analysis

Beta-ketoenoles like **AB-1** and **Sila-AB-1** are known to exist as tautomeric equilibria between the keto-, ketoimine-, *E*-enol- and *Z*-enol forms which strongly dependents on the solvents and substituents.[67] It was found that in apolar solvents the equilibrium is shifted towards the keto-form, and in polar solvents towards the enol (E or Z) isomer. Due to the predominately hydrophobic nature of the binding pocket we selected the keto forms of the active principles **AB-1** and **Sila-AB-1** for our further modeling studies. **AB-1** and **Sila-AB-1** possess in the keto form chiral centers and consequently in the tautomeric equilibria the *R* as well as the *S* configurations exist. Both these configurations were included into our docking studies at the Qp site.

The superior poses were selected based on the Glide-Score values and from binding mode analysis and it was found that binding of **AB-1** and **Sila-AB-1** to the Qp site in the *R* configuration of the keto form is strongly preferred to binding in the corresponding *S* configuration. Both compounds formed two hydrogen bonds with the residues of Trp165 and Tyr433 and the corresponding distances are 2.2 Å and 2.0 Å, respectively (Fig.4). The *tert*-butylbenzene or trimethylsilylbenzene moieties were located in the flexible pocket. Furthermore cation-π interactions were observed in 2D interaction diagrams (see Supporting imformation Fig. S1) between the trifluoromethyl-benzene ring and the residue of Arg279.

Our work demonstrated that **AB-1** and its sila-analogue **Sila-AB-1** bind in the same

conformation to *T. cinnabarinus* SQR. Interestingly, also in the binding modes research of SDHI fungicides, it was observed that two hydrogen bonds and a cation-π interactions were found with the residues of Trp, Tyr and Arg, respectively.[39, 62, 68] Our results indicate that high similarities and conserved ligand binding regions among acaricidal and fungicidal succinate dehydrogenase inhibitors and confirmed the important roles of residues Trp, Tyr and Arg in ligand-receptor interaction.

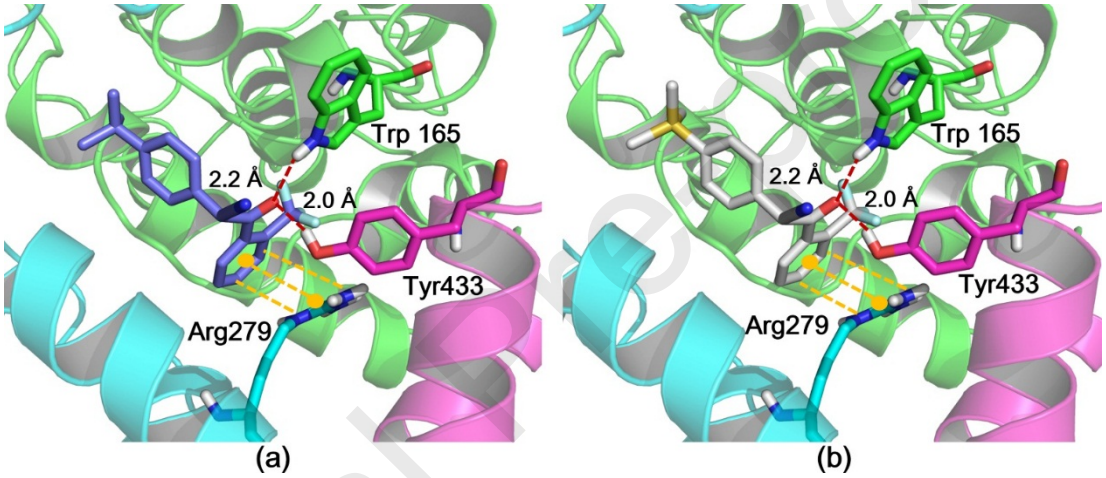

Fig. 4. The 3D binding mode of AB-1 (a) and its sila-analogue (b) with *T. cinnabarinus* SQR

3. Conclusions

The application of a carbon-silicon bioisosteric replacement strategy has resulted in the discovery Sila-Cyflumetofen, a novel and highly potent acaricide. We found that the *t*-butyl group of the *beta*-ketonitrile acaricide Cyflumetofen can be replaced by a trimethyl-silyl group with retention of high level acaricidal activity and favourable pharmacological properties.

The carbon-silicon replacement in Cyflumetofen was rationalized by potential

surfaces modeling and physicochemical properties analysis. Sila-Cyflumetofen retained similar preferred energy-minimized conformation, electrostatic potential surface and clogS compare to the parent compound. Although there were some changes in clogP values, the physicochemical properties of Sila-Cyflumetofen are still located in the ideal range observed for the commercial products.

Furthermore, we developed as part of our research a new mode of action test for Complex II acaricides using cytochrome c as electron acceptor and blocking its re-oxidation by addition of KCN resulting in a sensitive and convenient colorimetric assay that avoids the use of non-specific artificial electron acceptors and allows assay of SQR inhibition in crude extracts of *Tetranychus urtice*.

The acaricidal activity indicated that Sila-Cyflumetofen showed somewhat lower activity at 12.5 ppm than its carbon counterpart, however, in the enzyme inhibition assay the intrinsically active form of Sila-Cyflumetofen **Sila-AB-1,** exhibited stronger enzyme inhibition than the intrinsically active metabolite of Cyflumetofen **AB-1**, demonstrating that the somewhat lower acaricidal activity of Sila-Cyflumetofen in laboratory assays results from changes in physicochemical properties or pharmacological and pharmacodynamic properties.

We also developed the first homology model of spider mite SQR. Our molecular docking studies revealed that the active principles of Cyflumetofen and its sila-analogue bind to the Qp site in same binding pose and that both compounds form two H-bonds and a cation-π interaction with Trp 165, Tyr 433 and Arg 279, respectively. In summary, our modeling work demonstrated that carbon-silicon replacement does not affect the

binding modes and offers basic insights for the design of novel analogues of Sila-Cyflumetofen with improved activity as well as for the *de-novo* design of novel chemistries targeting the Cyflumetofen binding pocket in Complex II. Our pharmacophore model is expected to be instrumental for our ongoing further research on Complex II acaricides as well as for other research groups in this area.

Although the value of carbon-silicon bioisosteric replacements has already been demonstrated in the past, this is to the best of our knowledge the first report of a successful application in crop protection research in the last two decades. It is hoped that our data presented here will inspire scientists to think of employing such carbon-silicon bioisosteric replacement strategy in their design of agrochemicals of the future.

4. Experimental section

4.1 Materials and methods

All the reagents were purchased from commercial vendors and used without further purification. Anhydrous solvents were dried with standard methods before use. The progresses of reactions were monitored by thin layer chromatography (TLC) analysis on pre-coated plates (silica gel GF254), and spots were visualized under ultraviolet (UV) light. All the compounds were purified by column chromatography on silica gel. Melting points were determined on Büchi B540 (Büchi Labortechnik AG, Flawil, Switzerland) melting point apparatus with an uncorrected thermometer. ^{1}H NMR, and ^{13}C NMR spectra were recorded on Bruker AM-400 spectrometer in $CDCl_3$ or DMSO-d_6 solution with tetramethylsilane as internal standard. High-resolution mass spectra (HRMS) were determined on XEVO G2 TOF (ESI) or GCT Premier (EI) instrument. The yields obtained by the experiments were all isolated yields.

4.1.1 Synthesis of (4-bromophenyl)trimethylsilane ***2***

1,4-dibromobenzene (**1)** (12.5mmol) was dissolved with anhydrous tetrahydrofuran (100 mL) in pre-dried Schlenk tube (charged with Argon) and cooled to -78 °C, then *n*-BuLi (2.5 M in hexane, 5 mL, 12.5mmol) was added dropwise. The solution was stirred at -78 °C for 2 h, then chlorotrimethylsilane (15 mmol) was added and the reaction was allowed to warm to room temperature gradually. Saturated NH_4Cl solution was added and the residue was taken up in ether twice. The combined organic layer was washed with brine and dried with Na_2SO_4, filtered and concentrated under reduced pressure. After column chromatography the target compound was obtained. Yield 64.7%, colorless oil. ^{1}H NMR (400 MHz, $CDCl_3$) δ 7.48 (d, J = 8.2 Hz, 2H), 7.37 (d, J = 8.3 Hz, 2H), 0.25 (s, 9H) ppm.

*4.1.2 Synthesis of 2-(4-(trimethylsilyl)phenyl)acetonitrile **3B***

$Pd_2(allyl)_2Cl_2$ (0.1 mmol), S-Phos (0.3 mmol), sodium cyanoacetate (7.5 mmol) were added to a pre-dried two-necked bottle. The bottle was then evacuated and filled with Argon. (4-bromophenyl)trimethylsilane (**2)** (5 mmol) and 15 mL anhydrous mesitylene were added with a syringe. The reaction mixture was stirred at room temperature for 15 minutes, and then in a preheated oil bath at 140 °C for 5 h. Upon completion of the reaction, the mixture was cooled to room temperature and filtered. The solvent was removed under reduced pressure. After column chromatography the target compound was obtained. Yield 73.2%, yellow oil. ^{1}H NMR (400 MHz, $CDCl_3$) δ 7.53 (d, J = 8.1 Hz, 2H), 7.32 (d, J = 8.1 Hz, 2H), 3.74 (s, 2H), 0.27 (s, 9H) ppm.

*4.1.3 General procedure for the synthesis of the substituted ethyl phenylcyanoacetate **4A** and **4B***

NaH (60% in mineral oil, 15 mmol) was added to 20 mL tetrahydrofuran at 0^0C, then the mixture was stirred under the same condition for few minutes. 10 mmol of phenylacetonitrile **3A** or **3B**, respectively, was added dropwise under stirring at 0^0C. After warming to room temperature, diethyl carbonate (12 mmol) was added slowly, and then the solution was stirred at 56 °C. The reaction progress was monitored by TLC. After complete disappearance of the starting material, the reaction was quenched

with water at 0°C. Diluted hydrochloric acid was added to keep the pH at 4-5. The aqueous phase was extracted with ethyl acetate twice. The combined organic layer was washed with brine and dried with Na_2SO_4, filtered and concentrated under reduced pressure. After column chromatography the target compounds were obtained.

*4.1.3.1 Ethyl 2-cyano-2-(4-(tert-butyl)phenyl)acetate (**4A**)* Yield 43.2%, yellow oil. ^{1}H NMR (400 MHz, $CDCl_3$) δ 7.48 – 7.35 (m, 4H), 4.69 (s, 1H), 4.24 (q, J = 7.1 Hz, 2H), 1.30 (d, J = 11.5 Hz, 12H) ppm

*4.1.3.2 Ethyl 2-cyano-2-(4-(trimethylsilyl)phenyl)acetate (**4B**)* Yield 72.8%, yellow oil.^{1}H NMR (400 MHz, $CDCl_3$) δ 7.57 (d, J = 8.2 Hz, 2H), 7.44 (d, J = 8.0 Hz, 2H), 4.70 (s, 1H), 4.31 – 4.18 (m, 2H), 1.29 (t, J = 7.1 Hz, 3H), 0.27 (s, 9H) ppm

*4.1.4 General procedure for the synthesis of the substituted 2-methoxyethyl phenylcyanoacetate **5A** and **5B***

Ethyl phenylcyanoacetate **4A** or **4B** (3 mmol), respectively, and catalytic amount of H_2SO_4 were mixed in 10 mL 2-methoxyethanol. The reaction mixture was stirred at 120 °C and the reaction progress was monitored by TLC. Upon completion the reaction, the mixture was poured into 20 mL water and extracted with ethyl acetate twice. The organic layer was washed with saturated $NaHCO_3$ solution and dried with Na_2SO_4, filtered, and concentrated under reduced pressure. After column chromatography the target compounds were obtained.

*4.1.4.1 2-methoxyethyl 2-cyano-2-(4-(tert-butyl)phenyl)acetate (**5A**)* Yield 55.3%, light yellow oil. ^{1}H NMR (400 MHz, $CDCl_3$) δ 7.41 (q, J = 8.6Hz, 4H), 4.75 (s, 1H), 4.41-4.25 (m, 2H), 3.59 (t, J =5.3Hz, 2H), 3.33 (s, 3H), 1.32 (S, 9H) ppm

*4.1.4.2 2-methoxyethyl 2-cyano-2-(4-(trimethylsilyl)phenyl)acetate (**5B**)* Yield 73.2%, light yellow oil. ^{1}H NMR (400 MHz, $CDCl_3$) δ 7.56 (d, J = 8.2 Hz, 2H), 7.45 (d, J = 8.0 Hz, 2H), 4.77 (s, 1H), 4.41 – 4.25 (m, 2H), 3.59 (t, J = 5.4 Hz, 2H), 3.33 (s, 3H), 0.27 (s, 9H) ppm

*4.1.5 General procedure for the synthesis of cyflumetofen **6A** and sila-Cyflumetofen **6B***

NaH (60% in mineral oil, 1.5 mmol) and 3 mL tetrahydrofuran were mixed homogeneously at 0 °C , then 1 mmol of 2-methoxyethyl phenylcyanoacetate **5A** or 5**B**, respectively, and 2-(trifluoromethyl)benzoyl chloride (1.2 mmol) were added dropwise to the suspension and the resulting reaction mixture was stirred overnight at room temperature. The reaction was quenched with water at 0^0C, then diluted hydrochloric acid was added to keep the pH at 6-7. The aqueous phase was extracted with ethyl acetate twice. The combined organic layer was washed with brine and dried with Na_2SO_4, filtered and concentrated under reduced pressure. After column chromatography the target compounds were obtained.

*4.1.5.1 Cyflumetofen (**6A**)* Yield 62.5%, white solid, mp 77.3-80.7 °C. ^{1}H NMR (400 MHz, $CDCl_3$) δ 7.78 (d, J = 7.9 Hz, 1H), 7.60 (dd, J = 13.4, 8.2 Hz, 3H), 7.53 - 7.43 (m, 3H), 7.15 (d, J = 7.8 Hz, 1H), 4.54 - 4.35 (m, 2H), 3.64 (t, J = 4.8 Hz, 2H), 3.36 (s, 3H), 1.35 (s, 9H) ppm (mixture of conformers). ^{13}C NMR (100 MHz, $CDCl_3$) δ 189.8, 163.3, 153.2, 134.9, 131.4, 129.2,128.9, 128.6, 128.3(q, $^2J_{CF}$ = 32.4 Hz), 127.7, 127.3, 127.3, 127.2, 127.2(q, $^3J_{CF}$ = 4.8 Hz), 127.1, 126.2, 125.9, 124.4, 121.7 (d, $^1J_{CF}$ = 272.4 Hz), 115.2, 69.6, 66.93, 65.6, 59.0, 34.7, 31.2 ppm (mixture of conformers). HRMS (ESI) Calcd. for $C_{24}H_{24}F_3NO_4$+Na^+ $[M+Na]^+$ 470.1554; found 470.1556.

*4.1.5.2 Sila-Cyflumetofen (**6B**)* Yield 38.7%, white solid, mp 56.3-58.8 °C. ^{1}H NMR (400 MHz, $CDCl_3$,) δ 7.79 (d, J = 7.9 Hz, 1H), 7.66 – 7.56 (m, 5H), 7.49 (t, J = 7.6 Hz, 1H), 7.16 (d, J = 7.8 Hz, 1H), 4.54 – 4.35 (m, 2H), 3.64 (t, J = 4.8 Hz, 2H), 3.36 (s, 3H), 0.30 (s, 9H) ppm (mixture of conformers). ^{13}C NMR (100 MHz, $CDCl_3$) δ 190.9, 164.5, 144.3, 136.1, 135.5, 132.8, 130.6, 130.2, 129.9 (q, $^2J_{CF}$ = 32.3 Hz), 128.7, 128.6, 128.6, 128.5 (q, $^3J_{CF}$ = 4.8 Hz), 128.3, 125.6, 122.9 (d, $^1J_{CF}$ = 272.5 Hz), 116.3, 70.8, 68.2, 67.2, 60.3, 0.0 ppm (mixture of conformers). HRMS (ESI) Calcd. for $C_{23}H_{24}F_3NO_4Si$+Na^+ $[M+Na]^+$ 486.1324; found 486.1325.

*4.1.6 Synthetic procedure for ethyl 2-(trifluoromethyl)benzoate **8***

In a 75 mL pressure tube, a mixture of 2-trifluoromethylbenzoic acid **7** (20 mmol), ethanol (60 mL) and catalytic amount of H_2SO_4 was heated to 120 °C for 12 h. Then the reaction mixture was cooled to room temperature and about 80% of the ethanol

solvent was removed under reduced pressure. The remaining mixture was then poured into 30 mL water, neutralize with saturated $NaHCO_3$ solution, and extracted with ethyl acetate twice. The combined organic layer was washed with brine and dried with Na_2SO_4, filtered and concentrated under reduced pressure. The crude was purified by column chromatography to afford 2-trifluoromethylethylbenzoate. Yield 87.2%, colorless oil. ^{1}H NMR (400 MHz, $CDCl_3$) δ 7.74 – 7.64 (m, 2H), 7.56 – 7.50 (m, 2H), 4.38 – 4.28 (m, 2H), 1.32 (d, J = 14.3 Hz, 3H).

*4.1.7 General procedure for the synthesis of the active metabolites **AB-1** and **Sila-AB-1***

NaH (60% in mineral oil, 2.5 mmol) was mixed with 10 mL tetrahydrofuran, then the mixture was stirred in ice bath and 2mmol of phenylacetonitrile **4A** or **4B,** respectively, was added dropwise. After warming up to room temperature, ethyl 2-(trifluoromethyl)benzoate (**8**) (2.5 mmol) was added slowly, and then the solution was stirred under reflux. The reaction progress was monitored by TLC. After complete disappearance of the starting material, the reaction was quenched with water at 0 °C. Diluted hydrochloric acid was added to keep the pH at 4-5. The aqueous phase was extracted with ethyl acetate twice. The combined organic layer was washed with brine and dried with Na_2SO_4, filtered and concentrated under reduced pressure. The target compounds were obtained through recrystallization.

*The metabolite **AB-1*** Yield 64.2%, white solid, mp 161.4-164.2 °C. ^{1}H NMR (400 MHz, $CDCl_3$) δ 7.76 (dd, J = 19.1, 7.8 Hz, 3H), 7.69 – 7.48 (m, 16H), 7.39 (d, J = 8.4 Hz, 2H), 7.24 (d, J = 8.4 Hz, 2H), 7.15 (s, 1H), 5.21 (s, 1H), 1.35 (s, 18H), 1.30 (s, 9H), 1.22 (s, 1H). ^{13}C NMR (100 MHz, $CDCl_3$) δ 192.6, 162.6, 152.8, 151.9, 135.9, 132.40 132.3, 131.8, 131.2, 131.0, 128.3, 128.0, 127.9, 127.6, 127.1, 127.0, 126.9, 126.8, 126.8, 126.5, 126.3, 125.7, 118.4, 115.7, 93.1, 50.4, 34.7, 31.2, 31.2. HRMS (ESI) Calcd. for $C_{20}H_{18}F_3NO+Na^+$ $[M+Na]^+$ 368.1237; found 368.1239.

*The metabolite **Sila-AB-1*** Yield 51.7%, white solid, mp 143.7-146.1 °C. ^{1}H NMR (400 MHz, $CDCl_3$) δ 7.79 (dd, J = 16.0, 7.7 Hz, 4H), 7.66 (q, J = 7.0 Hz, 17H), 7.56 (t, J = 8.8 Hz, 4H), 7.32 (d, J = 7.9 Hz, 2H), 7.19 (s, 1H), 5.25 (s, 1H), 0.32 (s, 18H), 0.29 (s, 10H), 0.21 (s, 1H). ^{13}C NMR (100 MHz, $CDCl_3$) δ 193.7, 164.2, 143.8, 142.9, 137.1,

135.7, 135.5, 134.7, 133.6, 133.1, 133.0, 132.6, 132.3, 132.3, 132.1, 132.1, 130.3, 129.2, 129.0, 128.9, 128.6, 128.3, 128.3, 128.2, 128.1, 119.5, 116.7, 94.6, 52.0, 0.0, 0.0. HRMS (ESI) Calcd. for $C_{19}H_{18}F_3NOSi+Na^+$ $[M+Na]^+$ 384.1007; found 384.1006.

*4.1.8 General procedure for the synthesis of acylated derivatives **9A** and **9B***

AB-1 or **Sila-AB-1** (1 mmol), respectively, was dissolved in dichloromethane and then triethylamine (1.2 mmol) was added dropwise. After stirring under room temperature for 10 minutes, pivaloyl chloride (1.2 mmol) was added slowly. The reaction progress was monitored by TLC. After complete disappearance of the starting material, the reaction mixture was evaporated under reduced pressure, and the crude product was poured into water and the resulting mixture was extracted with ethyl acetate. The combined organic layer was washed with brine and dried with Na_2SO_4, filtered and concentrated under reduced pressure. After column chromatography the target compound was obtained.

*4.1.8.1 (2E)-3-(2,2-Dimethypropanoyloxy)-2-(4-tert-butylphenyl)-3-(2-trifluoromethyl phenyl)-acrylonitrile **(9A)*** Yield 62.7%, white solid, mp 85.3-88.5°C. ^{1}H NMR (400 MHz, $CDCl_3$) δ 7.80 (d, J = 7.5 Hz, 1H), 7.70 (d, J = 7.8 Hz, 1H), 7.61 (t, J = 7.4 Hz, 1H), 7.54 (t, J = 7.6 Hz, 1H), 7.45 – 7.35 (m, 4H), 1.26 (s, 9H), 0.98 (s, 9H). ^{13}C NMR (100 MHz, $CDCl_3$) δ 175.0, 157.5, 152.9, 132.9, 132.0, 131.3, 130.7, 128.9,128.5 (d, $^2J_{CF}$ = 32.2 Hz), 128.4, 127.2, 126.8, 126.8, 126.7, 126.7 (q, $^3J_{CF}$ = 4.9 Hz), 125.6, 125.0, 122.3 (d, $^1J_{CF}$ = 272.2 Hz), 116.8, 109.5, 39.1, 34.8, 31.2, 26.6. HRMS (EI): calcd for $C_{25}H_{26}F_3NO_2$ $[M]^+$ 429.1916, found 429.1917.

*4.1.8.1 (2E)-3-(2,2-Dimethypropanoyloxy)-2-(4-trimethylsilylphenyl)-3-(2-trifluoromethyl phenyl)-acrylonitrile **(9B)*** Yield 64.3%, white solid, mp 78.1-81.8 °C.^{1}H NMR (400 MHz, $CDCl_3$) δ 7.68 (d, J = 7.5 Hz, 1H), 7.58 (d, J = 7.7 Hz, 1H), 7.40 (ddd, J = 40.4, 21.5, 7.8 Hz, 6H), 0.85 (s, 9H), 0.09 (s, 9H). ^{13}C NMR (100 MHz, $CDCl_3$) δ 176.2, 159.3, 144.0, 134.8, 134.1, 133.3, 132.4, 132.1, 131.7, 130.4, 130.1, 129.8, 129.5 (q, ^2JCF = 31.2 Hz), 129.0, 128.9, 128.1, 128.1, 128.0, 128.0 (q, ^3JCF = 4.8 Hz), 127.9, 126.2, 123.5, 120.8 (q, ^1JCF = 272.2 Hz), 117.9, 110.9, 40.4, 27.8, 0.0. HRMS (EI): calcd for $C_{24}H_{26}F_3NO_2Si$ $[M]^+$ 445.1685, found 445.1684.

4.2 Biological assay

4.2.1 Acaricidal activities against two-spotted spider mite (Tetranychus urticae)

Bean leaf discs on agar in 24-well microtiter plates were sprayed with aqueous test solutions prepared from 10'000 ppm DMSO stock solutions. After drying the leaf discs were infested with a mite population of mixed ages. The samples were assessed for mortality on mixed population (mobile stages) 8 days after infestation.

4.2.2 Preparation of sub-mitochondrial particles from Tetranychus urticae

After 72 hours of infestation on bean plants, mites were collected by brushing, immediately frozen in liquid nitrogen and stored at -80°C. Sub-mitochondrial particles (SMP) were prepared at 4°C from 600 mg of mites. Mites were washed three times in 5 mM HEPES-KOH pH 7.4, 0.12 mM $MgCl_2$, 320 mM sucrose (buffer A), resuspended in 600 µl buffer A, and disrupted by sonication at 4°C using a Qsonica Q700 equipped with horn cup bath at amplitude 20, for 1 min. on 5 sec. on-off pulse cycle. The homogenate was filtered through cotton wool and centrifuged for 15 min at 10000 rpm in a Beckman Optima MAX-XP ultracentrifuge using a TLA-100.3 rotor. The supernatant was collected and membranes containing the SMP were recovered by centrifugation for 35 min. at 71000 rpm in a TLA-100.3 rotor. The resulting pellet was resuspended in buffer A, supplemented with 2 mM EDTA.

4.2.3 Assay of succinate-cytochrome oxidoreductase activity

The assay was essentially as described for mammalian tissues[69] and performed at room temperature. Serial dilutions of test compounds were prepared in 100% dimethyl sulfoxide (DMSO), and 1 µl dispensed from each dilution for each reaction. SMP were diluted to 0.15 mg/ml in reaction buffer (20 mM KH_2PO_4 pH 8.0) and 50 µl added to the reaction well followed by 50 µl 2 mM KCN in reaction buffer (to inhibit Complex IV activity) and 50 µl 32 mM cytochrome c in reaction buffer. After 15 mins the reaction was started by the addition of a further 50 µl of reaction buffer containing 12 mM succinate. The reduction of cytochrome c was monitored by the increase in optical

absorption at 550 nm. The initial rate of the reaction was fitted to a linear function. The IC50 values were calculated by fitting the dependence of the initial rates on compound concentration to a dose response model (y = min + ((max-min)/(1+10^(Hill(Log10(IC50))))) by nonlinear regression.

4.3 Potential Surfaces modeling and physicochemical properties analysis

Preferred energy-minimized conformations of Cyflumetofen and Sila-Cyflumetofen, optimized by Ligprep Module in Maestro 10.2 (Schrödinger, LLC, 2015), were used as inputs into Sybyl (Tripos Inc.). Potential Surfaces were created by MOLCAD Module. The color ramp for lipophilic potential surfaces range from brown (highest lipophilic area of the molecule) to blue (highest hydrophilic area). The color ramp for electrostatic potential surfaces range from red (most positive) to purple (most negative).

The clogP, clogS and TPSA of title compounds and commercial products were predicted by Canvas （Schrödinger, LLC, 2015）, ALOGPS 2.1 online server (http://www.vcclab.org/web/alogps/) and MOE (Molecular Operating Environment, version 2014). The experimental data of commercial products were retrieved from *The Pesticide Manual* and corresponding literature.[70] The detailed data were listed in Table S1 in Supporting information.

4.4 Homology modeling and molecualr docking

The target sequences of *T. cinnabarinus* SQR subunits B, C and D (UniProt ID: A0A0K1SB10, A0A0K1SB53 and A0A0K1SAS9) were retrieved from UniProt (http://www.uniprot.org/). The sequences were submitted to the National Center for Biotechnology Information (NCBI) (http://www.ncbi.nlm.nih.gov/) for template search using the BLAST program. The crystal structure of porcine heart Complex II co-crystalized with ubiquinone (PDB ID: 1ZOY, 2.4 Å resolution) was chosen as the template to build the 3D structures of *T. cinnabarin*us SQR eventually. The Prime program encoded in Maestro 10.2 was used to modulate sequence alignment manually. The Align Sequence to Template and Build Homology Models Modules encoded in the Discovery Studio 3.5 software package (Accelrys Inc., 2013) were applied to perform

the final sequence alignment and generate the *T. cinnabarinus* SQR structure. The iron-sulfur clusters, ubiquinone in Qp site and heme group were retained from the original template. Final geometric evaluation was performed on PROCHECK Ramachandran plot, Profile-3D and Prosa-web z-score approaches.

Preferred energy-minimized conformations of the two active principles were optimized by Ligprep Module in Maestro 10.2. Since the optimized conformations of the active forms **AB-1** and **Sila-AB-1** contained chiral centers, the *R* and *S* configurations were docked into the homology model simultaneously by Glide program with default settings in standard precision (SP) mode. The binding site was set around the centroid of the ubiquinone retained from the original template with a size of 15 Å. 100 conformations were output and ranked by Glide-Score in the ligand docking. The superior poses were selected for the further binding mode analysis.[71-72]

Acknowledgments

This work was financially supported by National Key Research and Development Plan (2017YFD0200300), the National Natural Science Foundation of China (21572059, 21977030), and Innovation Program of Shanghai Municipal Education Commission (201701070002E00037). Acaricidal activities and enzyme inhibition were measured at Syngenta. The authors would like to thank Patrik Hoegger and Gemma Hough for performing the biological testing.

Notes

The authors declare no competing financial interest.

Reference

1. Maienfisch, P.; Stevenson, T. M. Modern agribusiness-markets, companies, benefits and challenges. In *Discovery and Synthesis of Crop Protection Products*, *ACS Symp. Ser.*; Maienfisch, P., Stevenson, T. M., Eds.; American Chemical Society: Washington, DC, 2015; Vol. 1204, pp 1-13.

2. Sieburth, S. M.; Manly, C. J.; Gammon, D. W. Organosilane insecticides. Part I: biological and physical effects of isosteric replacement of silicon for carbon in etofenprox and MTI 800. *Pestic. Sci.* **1990**, *28*, 289-307.

3. Sieburth, S. M.; Langevine, C. N.; Dardaris, D. M. Organosilane insecticides. Part II: chemistry and structure-activity relationships. *Pestic. Sci.* **1990**, *28*, 309-319.

4. Koyanagi, T.; Haga, T. Bioisosterism in agrochemicals. In *Synthesis and Chemistry of Agrochemicals IV*, *ACS Symp. Ser.*; Don R. B., Joseph G. F., Gregory S. B., Eds.; American Chemical Society: Washington, DC, 1995; Vol. 584, pp 15-24.

5. Meanwell, N. A. Synopsis of some recent tactical application of bioisosteres in drug design. *J. Med. Chem.* **2011**, *54*, 2529-2591.

6. Langdon, S. R.; Ertl, P.; Brown, N. Bioisosteric Replacement and Scaffold Hopping in Lead Generation and Optimization. *Molecular informatics*. **2010**, *29*, 366-385.

7. Patani, G. A.; LaVoie, E. J. Bioisosterism: A rational approach in drug design. *Chem. Rev*. **1996**, *96*, 3147-3176.

8. Zhu, X.-Y.; Mardenborough, L. G.; Li, S.; Khan, A.; Zhang, W.; Fan, P.; Jacob, M.; Khan, S.; Walker, L.; Ablordeppey, S. Y. Synthesis and evaluation of isosteres of N-methyl indolo[3,2-b]-quinoline (cryptolepine) as new antiinfective agents. *Biorg. Med. Chem.* **2007**, *15*, 686-695.

9. Stockdale, D. P.; Beutler, J. A.; Wiemer, D. F. Synthesis of amide isosteres of schweinfurthin-based stilbenes. *Biorg. Med. Chem.* **2017**, *25*, 5483-5489.

10. Stockdale, D. P.; Titunick, M. B.; Biegler, J. M.; Reed, J. L.; Hartung, A. M.; Wiemer, D. F.; McLaughlin, P. J.; Neighbors, J. D. Selective opioid growth factor receptor antagonists based on a stilbene isostere. *Biorg. Med. Chem.* **2017**, *25*, 4464-4474.

11. Pasteris, R. J.; Hanagan, M. A.; Bisaha, J. J.; Finkelstein, B. L.; Hoffman, L. E.; Gregory, V.; Shepherd, C. P.; Andreassi, J. L.; Sweigard, J. A.; Klyashchitsky, B. A.; Henry, Y. T.; Berge, R. A. The discovery of oxathiapiprolin: a new, highly-active oomycete fungicide with a novel site of action. In *Discovery and Synthesis of Crop Protection Products, ACS Symp. Ser.;* Maienfisch, P., Stevenson, T. M., Eds.; American Chemical Society: Washington, DC, 2015; Vol. 1204, pp 149-161.

12. Pasteris, R. J.; Hanagan, M. A.; Bisaha, J. J.; Finkelstein, B. L.; Hoffman, L. E.; Gregory, V.; Andreassi, J. L.; Sweigard, J. A.; Klyashchitsky, B. A.; Henry, Y. T.; Berge, R. A. Discovery of oxathiapiprolin, a new oomycete fungicide that targets an oxysterol binding protein. *Biorg. Med. Chem.* **2016**, *24*, 354-361.

13. Mutahi, M. W.; Nittoli, T.; Guo L.; Sieburth, S. M. Silicon-Based Metalloprotease Inhibitors: Synthesis and Evaluation of Silanol and Silanediol Peptide Analogues as Inhibitors of Angiotensin-Converting Enzyme. *J. Am. Chem. Soc.* **2002**, *124*, 7363-7375.

14. Showell, G. A.; Mills, J. S. Chemistry challenges in lead optimization: silicon isosteres in drug discovery. *Drug Discov. Today*. **2003**, *8*, 551-556.

15. Showell, G. A.; Barnes, M. J.; Daiss, J. O.; Mills, J. S.; Montana, J. G.; Tacke, R.; Warneck, J. B. (R)-sila-venlafaxine: a selective noradrenaline reuptake inhibitor for the treatment of emesis. *Bioorg. Med. Chem. Lett.* **2006**, *16*, 2555-2558.

16. Sieburth, S. M.; Chen, C.-A. Silanediol protease inhibitors: From conception to validation. *Eur. J. Org. Chem.* **2006**, *37*, 311-322.

17. Tacke, R.; Popp, F.; Muller, B.; Theis, B.; Burschka, C.; Hamacher, A.; Kassack, M. U.; Schepmann, D.; Wunsch, B.; Jurva, U.; Wellner, E. Sila-haloperidol, a silicon analogue of the dopamine (D2) receptor antagonist haloperidol: synthesis, pharmacological properties, and metabolic fate. *Chemmedchem*. **2008**, *3*, 152-164.

18. Arnold, S. M.; Rinehart, J. J.; Tsakalozou, E.; Eckardt, J. R.; Fields, S. Z.; Shelton, B. J.; DeSimone, P. A.; Kee, B. K.; Moscow, J. A.; Leggas, M. A phase I study of 7-t-butyldimethylsilyl-10-hydroxycamptothecin in adult patients with refractory or metastatic solid malignancies. *Clin. Cancer. Res.* **2010**, *16*, 673-680.

19. Franz, A. K.; Wilson, S. O. Organosilicon molecules with medicinal applications. *J. Med. Chem.* **2013**, *56*, 388-405.

20. Ramesh, R.; Reddy, D. S. Quest for Novel Chemical Entities through Incorporation of Silicon in Drug Scaffolds. *J. Med. Chem.* **2018**, *61*, 3779-3798.

21. Moberg, W. K. Fungicidal 1-(silylmethyl)-1,2,4-triazole derivatives. EP Patent 4510136A, 1985.

22. Moberg, W. K. Fungicidal 1,2,4-triazole and imidazole derivatives. EP Patent

68813A2, 1983.

23. Tacke, R.; Becker, B.; Schomburg, D. The synthesis and the crystal and molecular structure of the fungicide bis(4-fluorophenyl)-methyl (1H-1,2,4-triazol-1-yl-methyl) silane (flusilazole, DPX H 6573). *Appl. Organomet. Chem.* **1989**, *3*, 133-139.

24. Schubert, H. H.; Salbeck, G.; Lueders, W.; Knauf, W.; Waltersdorfer, A. Silane derivatives, process for their preparation, agents containing them and their use as pesticides. EP Patent 224024A1, 1987.

25. Tacke, R.; Doerrich, S. Drug design based on the carbon/silicon switch strategy. *Top. Med. Chem.* **2016**, *17*, 29-59.

26. Sieburth, S.; Lin, S. Y.; Cullen, T. G. New insecticides by replacement of carbon by other group IV elements. *Pestic. Sci.* **1990**, *29*, 215-225.

27. Seetharamsingh, B.; Ramesh, R.; Dange, S. S.; Khairnar, P. V.; Singhal, S.; Upadhyay, D.; Veeraraghavan, S.; Viswanadha, S.; Vakkalanka, S.; Reddy, D. S. Design, Synthesis, and Identification of Silicon Incorporated Oxazolidinone Antibiotics with Improved Brain Exposure. *ACS Med. Chem. Lett.* **2015**, *6*, 1105-1110.

28. Yeh, T. K.; Li, C. M.; Chen, C. P.; Chuu, J. J.; Huang, C. L.; Wang, H. S.; Shen, C. C.; Lee, T. Y.; Chang, C. Y.; Chang, C. M.; Chao, Y. S.; Lin, C. T.; Chang, J. Y.; Chen, C. T. Antitumor activities and pharmacokinetics of silatecans DB-67 and DB-91. *Pharmacol. Res.* **2010**, *61*, 108-115.

29. Takahashi, N.; Nakagawa, H.; Sasama, Y.; Ikemi, N. Development of a new acaricide, cyflumetofen. *J. Pestic. Sci.* **2012**, *37*, 263-264.

30. Hayashi, N.; Sasama, Y.; Takahashi, N.; Ikemi, N. Cyflumetofen, a novel acaricide - its mode of action and selectivity. *Pest Manag Sci*. **2013**, *69*, 1080-1084.

31. Jeschke, P. Propesticides and their use as agrochemicals. *Pest Manag Sci*. **2016**, *72*, 210-225.

32. Khalighi, M.; Tirry, L.; Van Leeuwen, T. Cross-resistance risk of the novel complex II inhibitors cyenopyrafen and cyflumetofen in resistant strains of the two-spotted spider mite Tetranychus urticae. *Pest Manag Sci*. **2014**, *70*, 365-368.

33. Yu, H.-B; Cheng, Y.; Xu, M.; Song, Y.-Q; Luo, Y.-M; Li, B. Synthesis, Acaricidal Activity, and Structure-Activity Relationships of Pyrazolyl Acrylonitrile Derivatives.

J. Agric. Food Chem. **2016**, *64*, 9586-9591.

34. Khalighi, M.; Dermauw, W.; Wybouw, N.; Bajda, S.; Osakabe, M.; Tirry, L.; Van Leeuwen, T. Molecular analysis of cyenopyrafen resistance in the two-spotted spider mite Tetranychus urticae. *Pest Manage. Sci.* **2016**, *72*, 103-112.

35. Sugimoto, N.; Osakabe, M. Cross-resistance between cyenopyrafen and pyridaben in the twospotted spider mite Tetranychus urticae (Acari: Tetranychidae). *Pest Manage. Sci.* **2014**, *70*, 1090-1096.

36. Furuya, T.; Suwa, A.; Nakano, M.; Fujioka, S.; Yasokawa, N.; Machiya, K. Synthesis and biological activity of a novel acaricide, pyflubumide. *J. Pestic. Sci.*. **2015**, *40*, 38-43.

37. Nakano, M.; Yasokawa, N.; Suwa, A.; Fujioka, S.; Furuya, T.; Sakata, K. Mode of action of novel acaricide pyflubumide: effects on the mitochondrial respiratory chain. *J. Pestic. Sci*. **2015**, *40*, 19-24.

38. Yao, T.-T.; Xiao, D.-X.; Li, Z.-S.; Cheng, J.-L.; Fang, S.-W.; Du, Y.-J.; Zhao, J.-H.; Dong, X.-W.; Zhu, G.-N. Design, Synthesis, and Fungicidal Evaluation of Novel Pyrazole-furan and Pyrazole-pyrrole Carboxamide as Succinate Dehydrogenase Inhibitors. *J. Agric. Food Chem.* **2017**, *65*, 5397-5403.

39. Xiong, L.; Li, H.; Jiang, L.-N.; Ge, J.-M.; Yang, W.-C.; Zhu, X. L.; Yang, G.-F. Structure-Based Discovery of Potential Fungicides as Succinate Ubiquinone Oxidoreductase Inhibitors. *J. Agric. Food Chem.* **2017**, *65*, 1021-1029.

40. Xiong, L.; Zhu, X.-L.; Gao, H.-W.; Fu, Y.; Hu, S.-Q.; Jiang, L.-N.; Yang, W.-C.; Yang, G.-F. Discovery of Potent Succinate-Ubiquinone Oxidoreductase Inhibitors via Pharmacophore-linked Fragment Virtual Screening Approach. *J. Agric. Food Chem.* **2016**, *64*, 4830-4837.

41. Li, S.-K; Li, D.-D; Xiao, T.-F; Zhang, S.-S; Song, Z.-H; Ma, H-Y. Design, Synthesis, Fungicidal Activity, and Unexpected Docking Model of the First Chiral Boscalid Analogues Containing Oxazolines. *J. Agric. Food Chem.* **2016**, *64*, 8927-8934.

42. Tacke, R.; Heinrich, T.; Kornek, T.; Merget, M.; Wagner, S. A.; Gross, J.; Keim, C.; Lambrecht, G.; Mutschler, E.; Beckerss, T.; Bernd, M.; Reissmann, T. Bioorganogermanium Chemistry: Studies on C/Si/Ge Bioisosterism. *Phosphorus,*

Sulfur, and Silicon and the Related Elements. **1999**, *150*, 69-87.

43. Lazareva, N. F.; Lazarev, I. M. Drug design based on the carbon/silicon switch strategy. *Russ. Chem. Bull.* **2015**, *64*, 1221-1232.

44. Pooni, P. K.; Showell, G. A. Silicon switches of marketed drugs. *Mini Rev. Med. Chem.* **2006**, *6*, 1169.

45. Luger, P.; Dittrich, B.; Tacke, R. Invariom based electron density studies on the C/Si analogues haloperidol/sila-haloperidol and venlafaxine/sila-venlafaxine. *Org Biomol Chem*. **2015**, *13*, 9093-9106.

46. Shang, R.; Ji, D.-S.; Chu, L.; Fu, Y.; Liu, L. Synthesis of α-Aryl Nitriles through Palladium-Catalyzed Decarboxylative Coupling of Cyanoacetate Salts with Aryl Halides and Triflates. *Angew. Chem. Int. Ed.* **2011**, *50*, 4470-4474.

47. Takahashi, N.; Gotoda, S.; Ishii, N.; Sasama, Y. Preparation of benzoylcyanoacetic acid esters as miticides. PCT Int. Appl. WO 2002014263A1, 2002.

48. Compton, D. R.; Carlson, K. E.; Katzenellenbogen, J. A. Pyrazolo[1,5-a]pyrimidines as estrogen receptor ligands: defining the orientation of a novel heterocyclic core. *Bioorg. Med. Chem. Lett.* **2004**, *14*, 5681-5684.

49. Hoque, M. E.; Bisht, R.; Haldar, C.; Chattopadhyay, B. Noncovalent interactions in Ir-catalyzed C-H activation: L-shaped ligand for para-selective borylation of aromatic esters. *J. Am. Chem. Soc.* **2017**, *139*, 7745-7748.

50. Xu, F.-Z.; Wang, Y.-Y.; Luo, D.-X.; Yu, G.; Guo, S.-X.; Fu, H.; Zhao, Y.-H.; Wu, J. Design, synthesis, insecticidal activity and 3D-QSR study for novel trifluoromethyl pyridine derivatives containing an 1,3,4-oxadiazole moiety. *RSC Advances*. **2018**, *8*, 6306-6314.

51. Cao, S.-W; Liu, A.-P; Liu, W.-D; Liu, X.-P; Ren, Y.-G; Pei, H.; Huang, L.; Zheng, X.; Huang, M.-Z; Wu, D.-X. Synthesis and Insecticidal Activity of Novel Thiazole Acrylonitrile Derivatives. *J. Heterocycl. Chem.* **2017**, *54*, 3395-3402.

52. Huang, D.-L; Huang, M.-Z; Liu, A.-P; Liu, X.-P; Liu, W.-D; Chen, X.-Y; Xue, H.-S; Sun, J.; Yin, D.-L; Wang, X.-G. Design, Synthesis, and Acaricidal Activities of Novel Pyrazole Acrylonitrile Compounds. *J. Heterocycl. Chem.* **2017**, *54*, 9586-9591.

53. Earley, F. The Biochemistry of Oxidative Phosphorylation: A Multiplicity of

Targets for Crop Protection Chemistry. In *Modern Crop Protection Compounds*, Jeschke P.,Witschel M., Krämer W., Schirmer U., Eds.; Wiley-VCH: Weinheim, Germany, 2019; pp 609-633.

54. Jones, A. J. Y.; Hirst, J. A spectrophotometric coupled enzyme assay to measure the activity of succinate dehydrogenase. *Anal. Biochem.* **2013**, *442*, 19-23.

55. Wei, P.; Chen, M.; Nan, C.; Feng, K.-Y; Shen, G.-M; Cheng, J.-Q; He, L. Downregulation of carboxylesterase contributes to cyflumetofen resistance in Tetranychus cinnabarinus (Boisduval). *Pest Manage. Sci.* **2019**, *75*, 2166-2173.

56. Yankovskaya, V.; Horsefield, R.; Toernroth, S.; Luna-Chavez, C.; Miyoshi, H.; Leger, C.; Byrne, B.; Cecchini, G.; Iwata, S. Architecture of succinate dehydrogenase and reactive oxygen species generation. *Science*. **2003**, *299*, 700-704.

57. Horsefield, R.; Yankovskaya, V.; Sexton, G.; Whittingham, W.; Shiomi, K.; Omura, S.; Byrne, B.; Cecchini G.; and Iwata, S. Structural and Computational Analysis of the Quinone-binding Site of Complex II (Succinate-Ubiquinone Oxidoreductase). A Mechanism of Electron Transfer and Proton Conduction During Ubiquinone Reduction. *J. Biol. Chem.* **2006**, *281*, 7309-7316.

58. Ruprecht, J.; Yankovskaya, V.; Maklashina, E.; Iwata, S.; Cecchini, G. Structure of Escherichia coli Succinate:Quinone Oxidoreductase with an Occupied and Empty Quinone-binding Site. *J. Biol. Chem.* **2009**, *284,* 29836-29846.

59. Ruprecht, J.; Iwata, S.; Rothery, R. A.; Weiner, J. H.; Maklashina, E.; Cecchini, G. Perturbation of the Quinone-binding Site of Complex II Alters the Electronic Properties of the Proximal [3Fe-4S] Iron-Sulfur Cluster. *J. Biol. Chem.* **2011**, *286*, 12756-12765.

60. Sun, F.; Huo, X.; Zhai, Y.-J; Wang, A.-J; Xu, J.-X; Su, D.; Bartlam, M.; Rao, Z.-H Crystal Structure of Mitochondrial Respiratory Membrane Protein Complex II. *Cell*. **2005**, *121*, 1043-1057.

61. Zhou, Q.-J; Zhai, Y.-J; Lou, J.-Z; Liu, M.; Pang, X.-Y; Sun, F. Thiabendazole inhibits ubiquinone reduction activity of mitochondrial respiratory complex II via a water molecule mediated binding feature. *Protein & Cell*. **2011**, *2*, 531-542.

62. Inaoka, D. K.; Shiba, T.; Sato, D.; Balogun, E. O.; Sasaki, T.; Nagahama, M.; Oda, M.; Matsuoka, S.; Ohmori, J.; Honma, T.; Inoue, M.; Kita, K.; Harada, S. Structural

Insights into the Molecular Design of Flutolanil Derivatives Targeted for Fumarate Respiration of Parasite Mitochondria. *Int. J. Mol. Sci*. **2015**, *16*, 15287-15308.

63. Huang, L.-S.; Sun, G.; Cobessi, D.; Wang, A. C.; Shen, J. T.; Tung, E. Y.; Anderson, V. E.; Berry, E. A. 3-Nitropropionic Acid Is a Suicide Inhibitor of Mitochondrial Respiration That, upon Oxidation by Complex II, Forms a Covalent Adduct with a Catalytic Base Arginine in the Active Site of the Enzyme. *J. Biol. Chem.* **2006**, *281*, 5965-5972.

64. Huang, L.-S.; Shen, J. T.; Wang, A. C.; Berry, E. A. Crystallographic studies of the binding of ligands to the dicarboxylate site of Complex II, and the identity of the ligand in the "oxaloacetate-inhibited" state. *Biochim. Biophys. Acta*. **2006**, *1757*, 1073-1083.

65. Laskowski, R. A.; MacArthur, M. W.; Moss, D. S.; Thornton, J. M. PROCHECK: a program to check the stereochemical quality of protein structures. *J. Appl. Crystallogr.* **1993**, *26*, 283-291.

66. Eisenberg, D.; Luthy, R.; Bowie, J. U. VERIFY3D: assessment of protein models with three-dimensional profiles. *Methods Enzymol.* **1997**, *277*, 396-404.

67. Ruiz, D. L.; Albesa, A. G.; Ponzinibbio, A.; Allegretti, P. E.; Schiavoni, M. M., Solvent effects on tautomerics equilibria in β - ketonitriles: NMR and theoretical studies. *J. Phys. Org. Chem.* **2010**, *23*, 985-994.

68. Xiong, L.; Shen, Y.-Q.; Jiang, L.-N., Zhu, X.-L.; Yang, W.-C.; Huang, W.; Yang, G.-F Succinate dehydrogenase: an ideal target for fungicide discovery. In *Discovery and Synthesis of Crop Protection Products, ACS Symp. Ser.;* Maienfisch, P., Stevenson, T. M., Eds.; American Chemical Society: Washington, DC, 2015; Vol. 1204, pp 175-194.

69. Barrientos, A.; Fontanesi, F.; Diaz, F. Evaluation of the mitochondrial respiratory chain and oxidative phosphorylation system using polarography and spectrophotometric enzyme assays. *Curr Protoc Hum Genet*. **2009**, Chapter 19 Unit 19.3.1-19.3.14.

70. Zhang, Y.; Lorsbach, B. A.; Castetter, S.; Lambert, W. T.; Kister, J.; Wang, N. X.; Klittich, C. J. R.; Roth, J.; Sparks, T. C.; Loso, M. R. Physicochemical property guidelines for modern agrochemicals. *Pest Manage. Sci.* **2018**, *74*, 1979-1991.

71. Zheng, N.; Cheng, J.-G.; Zhang, W.; Li, W.-H.; Shao, X.-S.; Xu, Z.-P.; Xu, X.-Y.; Li, Z. Binding difference of fipronil with GABAARs in fruitfly and zebrafish: insights from homology modeling, docking, and molecular dynamics simulation studies. *J. Agric. Food Chem.* **2014**, *62*, 10646-10653.

72. Zhang, B.; Zhang, L.; He, L.-J.; Yang, X.-D.; Shi, Y.-L.; Liao, S.-W.; Yang, S.; Cheng, J.-G.; Ren, T.-R. Interactions of fipronil within fish and insects: experimental and molecular modeling studies. *J. Agric. Food Chem.* **2018**, *66*, 5756-5761.

Supporting Information

Design, synthesis and acaricidal activities of Cyflumetofen analogues based on carbon-silicon isosteric replacement

Cong Zhou[a], Jiagao Cheng[a,], Ryan Beadle[b,d], Fergus G Earley[b], Zhong Li[a], Peter Maienfisch[a,c]**

[a]*Shanghai Key Laboratory of Chemical Biology, School of Pharmacy, East China University of Science and Technology, Shanghai, 200237, China*

[b]*Syngenta Crop Protection AG, Jealott's Hill Research Centre, Bracknell, Berkshire, UK*

[c]*Syngenta Crop Protection AG, Schwarzwaldallee 215, CH-4002 Basel, Switzerland*

[d]*Current address: Department of Biochemistry, University of York, US*

* Corresponding authors: Peter Maienfisch, E-mail: peter.maienfisch@syngenta.com; Jiagao Cheng, E-mail: jgcheng@ecust.edu.cn

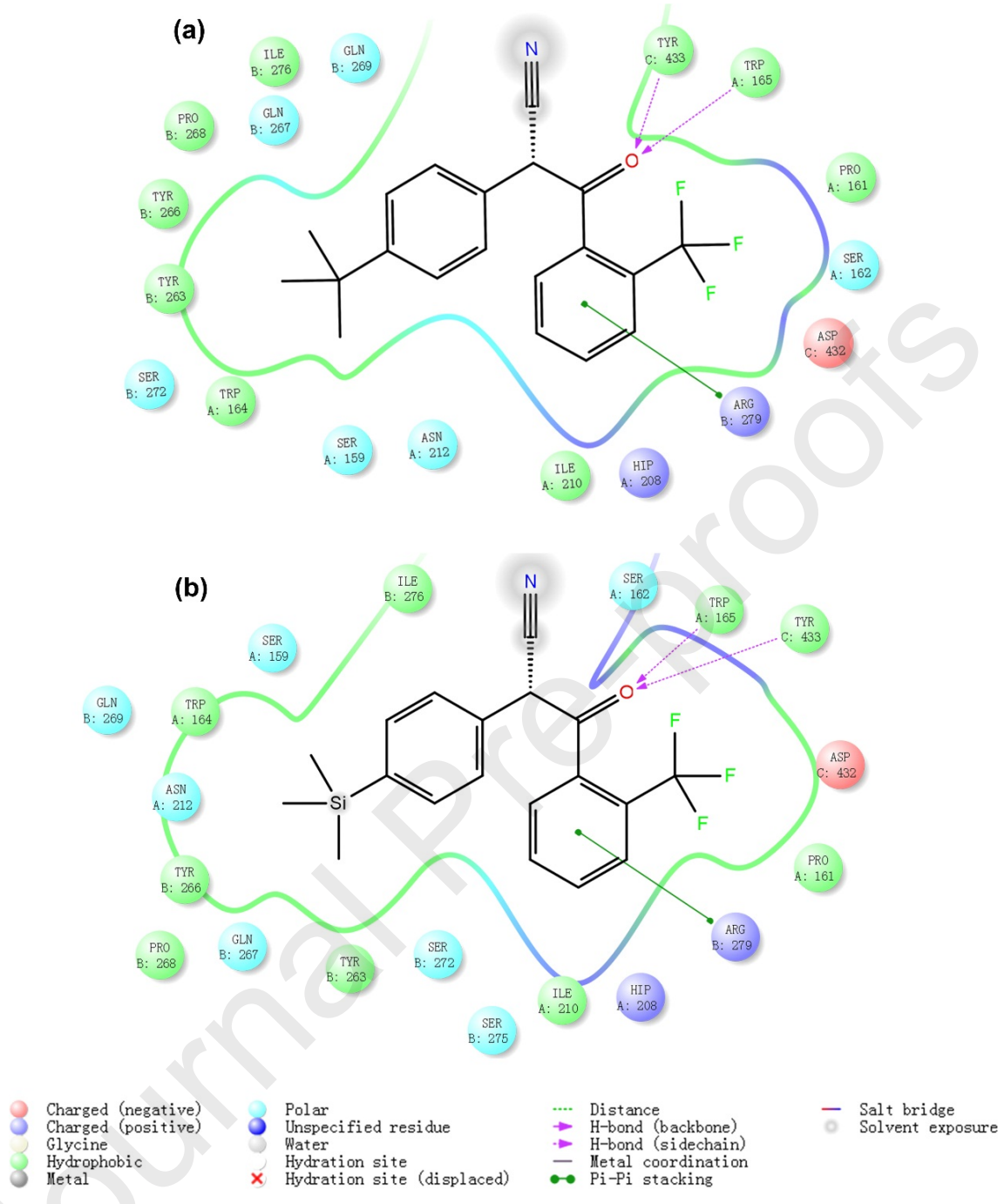

Fig. S1. The 2D binding mode of AB-1 (a) and its sila-analogue (b) with *T. cinnabarinus* SQR

Table S1. The detailed experimental and predicted physicochemical properties values of commercial products

	Experimental Values		Predicted values		
	logP	logS	clogP	clogS	TPSA
Bensultap	2.28	-0.35	3.88	-4.29	71.52
Bifenthrin	6	-3.00	6.37	-6.98	26.3
Broflanilide	5.7	-0.15	7.74	-5.24	49.41
Chlorantraniliprole	2.76	0.00	4.20	-5	88.91
Chromafenozide	4.83	-0.85	4.98	-5.2	58.64
Chlorfenapyr	2.7	-0.10	5.57	-5.2	37.95
Cyclaniliprole	2.7	-0.82	5.66	-5.61	88.91
Cypermethrin	6.94	-2.40	5.30	-5.68	59.32
Deltamethrin	4.6	-3.70	5.52	-5.61	59.32
Fenoxycarb	4.07	0.90	3.75	-4.03	56.79
Fipronil	4	0.28	5.53	-2.91	103.91
Flubendiamide	4.2	-1.52	5.30	-5.45	92.34
Flufenoxuron	4	-2.82	6.65	-5.94	67.43
Halofenozide	3.22	1.09	3.67	-5.03	49.41
Indoxacarb	4.65	-0.70	6.97	-5.41	106.97
lambda-Cyhalothrin	7	-2.30	5.79	-5.97	59.32
Lufenuron	5.12	-1.30	7.01	-5.57	67.43
Metaflumizone	4.7	-3.74	7.88	-5.29	86.51
Methoxyfenozide	3.7	0.52	4.45	-5.14	58.64
Novaluron	4.3	-3.52	7.27	-5.42	76.66
Noviflumuron	4.94	-0.71	7.22	-5.33	67.43
Pyridalyl	8.1	-3.82	6.51	-6.2	40.58
Pyriproxyfen	4.86	-0.43	4.77	-4.3	40.58
Spinetoram	4.1	1.04	5.26	-6.2	111.22
Spinosad	4	2.37	4.47	-5.53	111.22
Tebufenozide	4.25	-0.08	4.92	-5.49	49.41

Tebufenpyrad	4.93	0.42	4.24	-4.62	46.92
Teflubenzuron	4.3	-2.00	5.02	-5.57	58.2
Tolfenpyrad	5.61	-1.10	4.89	-5.16	56.15
Triflumuron	4.91	-1.60	5.65	-5.5	67.43
Acequinocyl	6.2	6.2	6.2	-6.48	60.44
Benomyl	1.37	0.46	3.59	-2.91	85.25
Benzoximate	2.4	1.48	4.22	-5.56	66.35
Bifenazate	3.4	0.31	3.87	-4.28	59.59
Bromopropylate	5.4	-0.30	4.84	-5.41	46.53
Chinomethionat	3.78	0.00	4.14	-2.67	42.85
Clofentezine	4.1	-2.60	4.21	-4.07	51.56
Cyenopyrafen	5.6	-0.52	5.45	-4.51	67.91
Cyflumetofen	4.3	-1.55	5.12	-5.58	76.39
Cyhexatin	4.86	0.00	-2.07	-5.33	20.23
Dichlofluanid	3.7	0.11	3.84	-3.83	40.62
Dicofol	4.3	-0.10	5.62	-5.56	20.23
Diflovidazin	3.7	-0.70	3.95	-4.09	51.56
Dinobuton	3.038	-1.00	4.41	-4.86	127.17
Dinocap	4.54	-0.82	5.85	-6.18	117.94
Etoxazole	5.59	-1.12	5.52	-4.86	30.82
Fenazaquin	5.51	-0.99	5.22	-5.51	35.01
Pyflubumide	5.2	-1.82	5.83	-5.21	64.43
Fenotiocarb	3.51	-1.47	3.58	-3.44	29.54
Fenpyroximate	5.01	-1.64	4.63	-5.41	74.94
Fluacrypyrim	4.51	-0.46	4.32	-4.37	79.77
Fluazuron	6.1	-1.70	6.50	-6.12	80.32
Hexythiazox	2.53	-0.30	5.61	-4.82	49.41
Propargite	5.7	-0.67	5.03	-4.31	63.97
Tertradifon	4.61	-1.11	5.59	-5.95	34.14
Pyridaben	6.37	-1.92	5.24	-4.31	32.67

Spirodiclofen	5.1	-0.72	6.38	-6.32	52.6
Spiromesifen	4.55	-0.89	5.64	-5.61	52.6
Acetamiprid	0.8	3.63	1.71	-3.1	52.28
Clothianidin	0.7	2.53	0.66	-3.25	95.13
Cyantraniliprole	1.94	1.15	3.41	-4.33	112.7
Dinotefuran	-0.55	4.60	-0.31	-1.98	91.47
Flonicamid	0.3	3.72	0.56	-3.52	65.78
Flupyradifurone	1.2	3.51	1.87	-2.13	42.43
Imidacloprid	0.57	2.79	1.05	-2.82	86.34
Nitenpyram	-0.66	4.00	1.70	-2.93	73.98
Pymetrozine	-0.18	2.46	0.29	-2.93	69.95
Pyrifluquinazon	3.12	1.08	3.67	-4.44	65.54
Spirotetramat	2.51	1.48	3.54	-4.39	73.86
Sulfoxaflor	0.8	2.76	2.00	-3.93	53.75
Thiacloprid	0.73	2.27	2.20	-2.74	52.28
Thiamethoxam	-0.13	3.61	0.73	-2.96	86.78
Triflumezopyrim	1.2	2.45	3.68	-6.04	66.17

Declaration of interests

☒ The authors declare that they have no known competing financial interests or personal relationships that could have appeared to influence the work reported in this paper.

☐The authors declare the following financial interests/personal relationships which may be considered as potential competing interests:

Peter Maenfisch
03 January 2020